Доклади на Българската академия на науките
Comptes rendus de l'Académie bulgare des Sciences

*Tome 72, No 3, 2019*

*SPACE SCIENCES*

*Space physics*

# GEOMAGNETIC FOCUSING OF COSMIC RAYS IN THE LOWER ATMOSPHERE – EVIDENCE AND MECHANISM

**Natalya A. Kilifarska, Rumiana Bojilova**

(*Submitted by Corresponding Member P. Velinov on January 18, 2019*)

**Abstract**

This paper shows that geomagnetic rigidity and the elevation of measurement point could not explain the irregularities found in the spatial distribution of annual mean cosmic ray radiation, detected by neutron monitors (NMs) spread over the world. Our theoretical analysis reveals that longitudinal gradient of heterogeneously distributed geomagnetic field could focus the extended showers of energetic particles in some regions of the Earth. We show that in regions with a positive, steeper rising cross-longitudinal magnetic gradient the NMs detect a higher annual mean radiation dose, compared to regions with a zero, or a negative magnetic gradient.

Moreover, we found out that the shape of the NMs' seasonal variations is confined to geographic latitude, and covariate fairly well with the lower stratospheric ozone ($O_3$), with an opposite phase. We hypothesise that this connectivity could be attributed to the ozone modulation of the mean free path of the cosmic rays' nuclei in the atmosphere and the muons production in the lower stratosphere.

**Key words:** neutron monitors, spatial and seasonal variations of near surface particles' fluxes, longitudinal drift in heterogeneous geomagnetic field

**PACS Numbers:** 07.77.Ka, 52.20.hv, 91.25.G, 92.60.hd, 94.20.Qq, 94.30.Hn, 96.50.S

This research is partially supported by the Bulgarian National fund for scientific research, project No Nt 14-28.

DOI:10.7546/CRABS.2019.03.11

**Introduction.** The flux of cosmic rays (CR) (of galactic or solar origin) approaching the outer boundary of Earth's magnetosphere are approximately homogeneous. Those of them which are coming along the open magnetic field lines are either repelled back in space by geomagnetic field, or are lost in the atmosphere due to the multiple collisions with atmospheric molecules. Particles approaching the closed magnetic field lines, whose energy is insufficient to overcome it, become trapped or quasi-trapped in geomagnetic field. Driven by the Lorentz force they start moving along the magnetic field lines on a spiral trajectory, continuously bouncing between the Northern and the Southern Hemispheres. Trapped particles, in addition, are drifting slowly across the magnetic field lines – repeatedly circling around the planet. They are making full revolution around the Earth for several minutes, up to several days, depending on their energy. The direction of protons' drift is toward the west, whereas that of the electrons – to the east. Although the resident time of the trapped particles could be quite long [1,2], the interaction with magnitospheric instabilities, plasma waves, etc., ensures a continuous spray of trapped particles in the lower, denser, atmosphere. Colliding with the atmospheric molecules, these particles produce secondary ions and electrons, as well as different products of nuclear reactions – some of them highly penetrating, being detected by the sea-level neutron monitors. The efficiency of the ion-molecular and nuclear reactions depends on the atmospheric characteristics such as density, temperature, humidity, etc. Thus for more than 70 years scientists have noticed the existing relation between the CRs' intensity near the Earth's surface and the lower stratospheric temperature and pressure [3–6].

Besides the meteorological influence, the seasonal variability of cosmic radiation is influenced by the geomagnetic field variations. Detailed analysis of the annual geomagnetic variability shows that only about 50% of it could be attributed to external factors [7]. The other 50% they attribute to the heterogeneous distribution of geomagnetic field over the globe.

This paper investigates the temporal and spatial variability of the near surface radiation measured by 33 neutron monitors (NMs), spread over the world. The found irregularities (being unexplainable in the framework of the magnetic rigidity-altitude dependence) are properly interpreted as an additional CR modulation by the irregularly distributed geomagnetic field, and its influence on the lower stratospheric ozone.

**Data and methods.** The temporal and spatial variability of galactic CR's – measured during 2009 at the ground surface – has been analysed in 33 neutron monitors, with freely available data at NMDB portal: `http://www01.nmdb.eu` or at IZMIRAN data server: `http://cr0.izmiran.ru/common/links.htm`. The analysed data are preliminarily corrected for influence of surface pressure and the monitors' efficiency.

Being a year of extremely low solar minimum, 2009 provides an opportunity for measurement of galactic cosmic radiation, which is less affected by the weak, uncompressed solar wind. Moreover, in periods of quiet Sun, the solar induced geomagnetic variability is also minimal. Consequently, in such a period it could be easier to detect both – the impact of geomagnetic heterogeneity (originating in the deviations of geomagnetic field from a dipole magnet), and the atmospheric influence on the secondary particles produced by CR in the atmosphere (due to CR interactions with stratospheric molecules), which are detected by the NMs.

In order to assess the effect of geomagnetic heterogeneity, we have analysed annual mean values of each NM. Analysis of the temporal variation has been done after extraction of the annual mean from each time record. The calculated difference is normalised by the annual mean, which allows a comparison of individual seasonal variability between different NMs.

Gridded data for a lower stratospheric temperature and ozone at 70 hPa has been taken from the ERA-Interim reanalysis `http://apps.ecmwf.int/datasets/data/interim-full-daily/levtype=sfc/`.

**Analysis of neutron monitors' annual means.** According to common understanding, the dominant part of particles reaching the Earth's surface arrives along the open magnetic field lines. This means that NMs with lower geomagnetic rigidity receive higher radiation dose than those situated at lower geomagnetic latitudes (i.e. with higher geomagnetic cutoff rigidity). The intensity of the measured particles' fluxes depends also on the altitude of the monitoring station, because only particles with very high energies are able to penetrate deeper in the atmosphere. To understand how these controversial factors affect the spatial distribution of the particles' intensity near the surface, we have combined two maps – the one showing the NMs' altitudes and the other – their annual mean counting rates. The result is presented in Fig. 1 (top panel) and it reveals that the dominant factor, determining the measured particles' intensity, is the altitude of the NM. It is easily visible that the highest particles' fluxes are observed in the monitors with higher elevation over the sea level.

On the other hand, a closer look to the mean particles' fluxes – detected by monitors with similar elevations above the sea level, but with different magnetic rigidity ($R_c$) – reveals some unexpected results. Thus, the annual mean impulses measured in Thule, Inuvik and Nain (all of them with $R_c = 0.3$) is almost twice smaller than the measured one in Moscow ($R_c = 2.43$) – refer to Table 1. Similarly, Table 1 shows that particles' intensity in Fort Smith ($R_c = 0.3$) is smaller than those measured in a station with 7 times higher magnetic rigidity – Magadan ($R_c = 2.1$), despite their similar elevations. Stations Tixie Bay ($R_c = 0.48$) and Norilsk ($R_c = 0.63$) – both being on the sea level, having similar latitudes and magnetic rigidities – count, however, substantially different particles' fluxes (in Norilsk being much higher than in Tixie Bay).

Another example, of the violation of our expectation for the determining role of NMs' altitude and magnetic rigidity, gives the comparison of the African stations – Tsumeb ($R_c = 9.15$) and Potchefsroom ($R_c = 6.98$). Table 1 shows

Table 1

List of analysed neutron monitors with their geographic coordinates, geomagnetic rigidity, elevation above sea level and annual mean value of measured cosmic ray flux

| NM code | Lat. [°] | Long [°] | Rigidity [GV] | Alt [m] | Ann. Mean |
|---|---|---|---|---|---|
| ATHN | 37.97N | 23.78E | 8.53 | 260 | 57.25152 |
| HRMS | 34.43S | 19.23E | 4.58 | 26 | 75.9217 |
| NEWK | 39.68N | 75.75W | 2.4 | 50 | 102.6935 |
| TXBT | 71.59N | 128.78E | 0.48 | 0 | 104.1229 |
| YKTS | 61.99N | 129.7E | 1.65 | 105 | 107.8079 |
| OULU | 65.05N | 25.47E | 0.81 | 15 | 113.405 |
| DRBS | 50.1N | 4.59E | 3.18 | 225 | 115.31 |
| INUVIK | 68.36N | 133.72W | 0.3 | 21 | 122.4717 |
| IRKS | 52.47N | 104.03E | 3.64 | 435 | 130.223 |
| THULE | 76.5N | 68.7W | 0.3 | 26 | 130.7371 |
| NAIN | 56.55N | 61.68W | 0.3 | 46 | 135.9816 |
| FRSM | 60.02N | 111.93W | 0.3 | 180 | 137.2711 |
| MGDN | 60.04N | 151.05E | 2.1 | 220 | 147.9627 |
| ROME | 41.86N | 12.47E | 6.27 | 0 | 158.1803 |
| MCMU | 77.9S | 166.6E | 0.3 | 48 | 174.7839 |
| SNAE | 70.17S | 2.35W | 0.73 | 856 | 178.7281 |
| KIEL | 54.34N | 10.12E | 2.36 | 54 | 180.407 |
| NRLK | 69.26N | 88.05E | 0.63 | 0 | 180.8299 |
| APTY | 67.57N | 33.39E | 0.65 | 181 | 185.5019 |
| KGSN | 42.98S | 147.29E | 1.88 | 65 | 219.3107 |
| KERG | 49.35S | 70.25E | 1.14 | 33 | 236.6656 |
| MOSC | 55.47N | 37.32E | 2.43 | 200 | 241.5492 |
| PTFM | 26.68S | 27.09E | 6.98 | 1351 | 59.36347 |
| AANM | 43.04N | 76.94E | 6.69 | 3340 | 167.3898 |
| JUNG | 46.55N | 7.98E | 4.49 | 3475 | 168.0818 |
| MXCO | 19.8N | 99.18W | 8.28 | 2274 | 232.7406 |
| TSMB | 19.2S | 17.58E | 9.15 | 1240 | 338.8673 |
| CALG | 51.08N | 114.13W | 1.08 | 1123 | 349.2115 |
| LMKS | 49.2N | 20.22E | 3.84 | 2634 | 471.998 |
| NANM | 40.37N | 44.25E | 7.1 | 2000 | 496.1897 |
| PSNM | 18.59N | 98.49E | 16.8 | 2565 | 620.3297 |
| ARNM | 40.47N | 47.44E | 7.1 | 3200 | 670.1337 |
| TIBT | 30.11N | 90.56E | 14.1 | 4300 | 3166.691 |

that the particles' flux intensity measured in the station with substantially higher magnetic rigidity (Tsumeb), is almost 6 times higher. Similar is the situation with stations Kerguelen ($R_c = 1.14$) and Sinae ($R_c = 0.73$) – the annual mean particles' flux in an elevated, with a lower rigidity station (Sinae) is much weaker.

These and many other "deviations" from the common understanding about the factors determining the intensity of particles reaching the Earth's surface, suggest that there might exist another factor(s) affecting the intensity of parti-

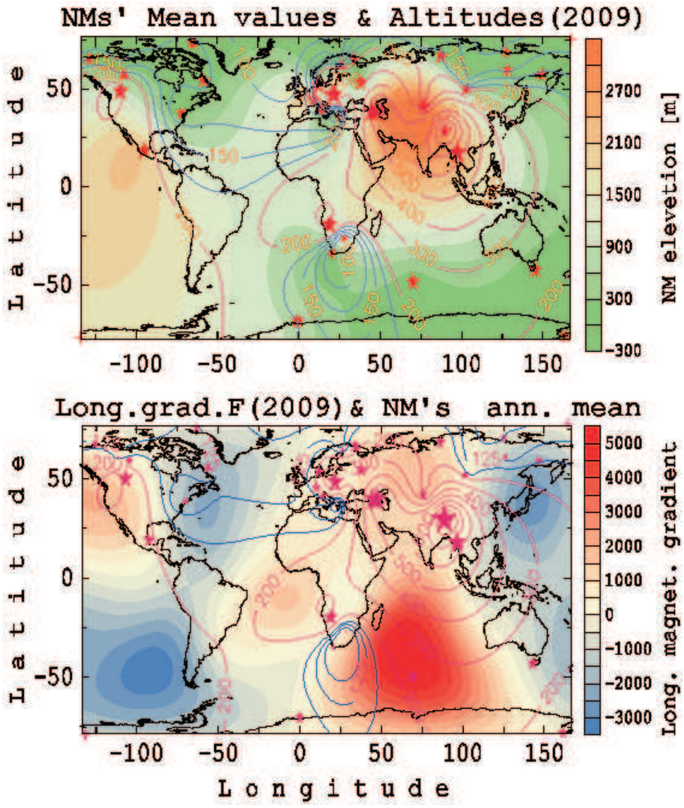


Fig. 1. (*coloured shading*): Maps of neutron monitors' (NMs) elevation above sea level (*top*) and longitudinal gradient of geomagnetic field (*bottom*). Overdrawn contours present the spatial distribution of annual mean counting rates for 2009, based on the individual values calculated for each NM

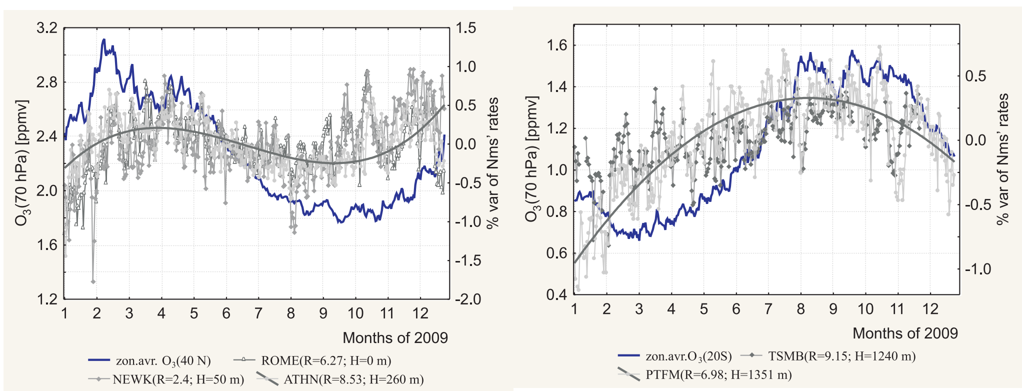


Fig. 3. Seasonal variations of neutron monitors' measurements, placed in regions with zero or slightly negative longitudinal magnetic gradient. Continuous blue lines illustrate the ozone mixing ration at 70 hPa

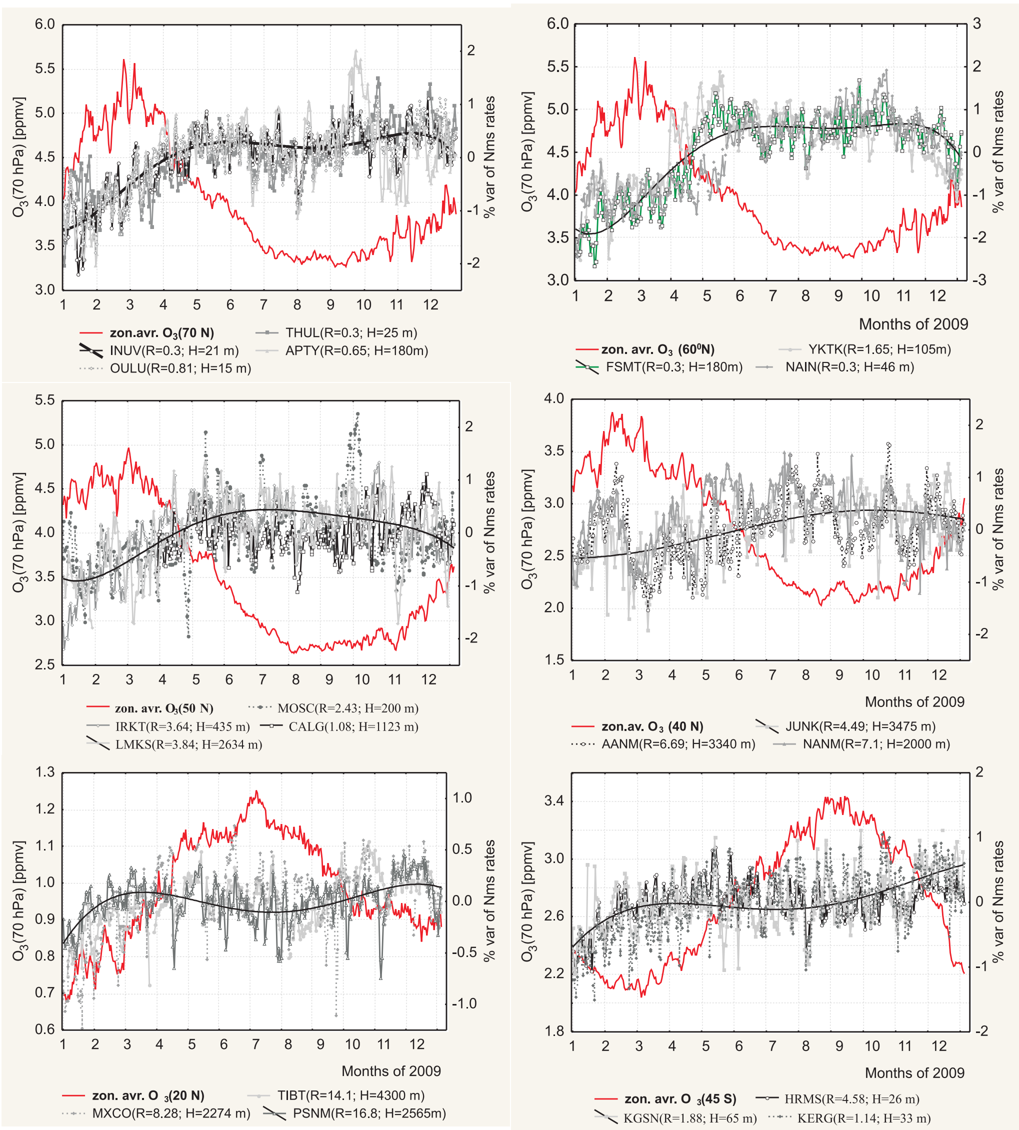


Fig. 2. Seasonal variation of near surface cosmic radiation (different grey-black symbols), measured by NMs at different latitudinal zones. The red contours show the seasonal variations of ozone mixing ration at 70 hPa for corresponding geographic latitudes. The thick continuous lines represent the polynomial fits to the daily values of CR measurements

cles' distribution over the globe. One such factor could be the trapped particles in the Earth's radiation belts. The following section will describe the possible mechanism of such an influence.

**Geomagnetic focusing of energetic particles in the lower atmosphere.** The geomagnetic field is a vector sum of the field of a dipole magnet, non-dipole part related to the heterogeneous structure of the deep Earth's interior, magnetic properties of the crustal rocks and magnetic field of external sources. The resultant vector at the planetary surface differs substantially from the dipole magnetic field and is accompanied by a non-uniform magnetic gradient – particularly in the direction perpendicular to the magnetic field lines. This means that when moving closer to the Earth surface, particles start feeling the magnetic irregularities (particularly in the lower part of their spiral motion along the magnetic field lines) [8–11], which in turn affect the speed of particles' longitudinal drift, determined by the formula (1):

$$\mathbf{v}_{\mathrm{drift}} = \frac{\mathbf{m}}{\mathrm{q}\cdot\mathrm{B}^2}\left(\mathrm{v}_\perp^2\cdot\frac{\mathrm{B}\times\nabla\mathbf{B}}{2\mathrm{B}} + \mathrm{v}_\parallel^2\cdot\frac{\boldsymbol{\rho}\times\mathrm{B}}{\rho^2}\right) \tag{1}$$

where $\mathbf{B}$ is the magnetic vector, $\boldsymbol{\rho}$ – magnetic field lines' curvature, $v_\parallel$ and $v_\perp$ are correspondingly the field aligned particles' speed and the velocity perpendicular to the geomagnetic field lines; **q** and **m** are particle's charge and mass, respectively. The first term in the brackets corresponds to the magnetic *gradient* perpendicular to the magnetic field lines, while the second term – to their *curvature*. Close to the point of the magnetic mirror, the field aligned particles' velocity is approaching zero, so the drift velocity is determined mainly by the cross-latitudinal and cross-longitudinal magnetic gradients.

Under the influence of the bi-directional magnetic gradient (in x-y plane, with x directed to the east, while y – to the north), the protons – entering the Earth's atmosphere from the west (in the lowest part of their circular trajectories) – are shifted south-westward, when entering regions with a positive cross-longitudinal gradient, and south-eastward – in regions with a negative gradient. Consequently, the overall *westward* drift (forced by the magnetic curvature and cross-latitudinal gradient) is reduced by the *eastward* component – exerted by the negative cross-longitudinal magnetic gradient in regions like East American-Atlantic region, Eastern Asia-Western Pacific and South Atlantic anomaly. Furthermore, the drift aligned electric field – expelling the confined particles outside the magnetic trap (due to the $(\mathrm{E}\times\mathrm{B})/\mathrm{B}^2$ electric drift) – is significantly reduced. As a result, in such regions only a few particles have a "chance" to be lost in the atmosphere, and the ground based neutron monitors should measure low counting rates.

Conversely, in regions with growing positive cross-longitudinal gradients (e.g. North-Western America and Eastern Europe-Western Asia) the south-westward component, induced by the cross-longitudinal magnetic gradient, increases the amplitude of the westward drift, impelled by the magnetic curvature and latitudinal gradient. Consequently, in these regions the drift induced charge separation, and related to them electric field, will intensively expel the charged particles outside the magnetic trap. Furthermore, these particles interact with the atmospheric molecules creating secondary electrons, ions and nuclear products, giving rise to the ionisation of the lower atmosphere, and to the radiation measured by the ground based neutron monitors.

The validity of these theoretical considerations is presented in the bottom panel of Fig. 1, which compares the maps of the longitudinal magnetic gradient (coloured shading) with annual mean values of NMs' counting rates (contours). Although the map of the near surface particles' intensity is quite rough (due to the relatively small number of neutron monitors and their irregular distribution over the globe), Fig. 1 fairly well shows that the lower counting rates are detected in regions with a negative or zero magnetic drift. This effect could be a reasonable explanation for the higher particles' intensity countered in Moscow – compared to Inuvik, Tule, Nain and other neighbours (Kiel, Oulu, Apatity). Similarly, the dose measured in Norilsk and Irkutsk (situated in a region with positive magnetic gradient) are higher than those detected in Tixie Bay, Yakutsk and Magadan – placed in a region with a decreasing (along the path of the arrival protons) magnetic field.

**Spatial distribution of the NM's seasonal variations.** Besides the annual mean values, we have also analysed the seasonal variation of all examined neutron monitors, which vary quite a lot between the individual stations. More detailed analysis reveals, however, that the shape of the seasonal variability is mostly confined to the geographic latitude (see Fig. 2). This implies that the seasonal variations of neutron monitors are more probably related to meteorological, instead of geomagnetic effects. Here it is worthy to remind that the data used are already corrected for the surface pressure variability, which means that some other atmospheric effect should influence the NMs' measurements.

Meanwhile, in the middle of the 20th century, some authors found out the dependence of CRs' seasonal variations on the atmospheric temperature between 50 and 100 hPa [3–5]. There is a maximum of stratospheric $\pi$-*mesons* production within the CR atmospheric showers [12], that is why Duperier [4] attributed the relation between the NM's counting rates and the lower stratospheric temperature to the following competing processes: 1) *mesons*' decay into *muons* – being the main atmospheric *source of muons*, and 2) nuclear capture of mesons through their interaction with other nuclei – acting as an stratospheric *sink of muons* [4]. The prevalence of any of these processes depends on the mesons' energy and the atmospheric density – determining the *mean free path* of atmospheric mesons ($d_\pi$), before their decay to muon and neutrino [13]. Thus, if the free path of atmospheric nuclei is greater than $d_\pi$, the mesons' decay is dominating, i.e. muons production. Otherwise the atmospheric mesons interact with atmospheric nuclei, producing tertiary, quaternary, etc. subatomic particles. Even if some of the newly appearing products is another meson, which furthermore succeeds to decay to a muon, the latter has much less energy and its probability to reach the Earth's surface is severely reduced [13].

Our comparative analysis of the NMs' counts and atmospheric temperature at 70 hPa reveals that at some latitudes (i.e. 30°–10°N and 30°–40°S, as well as over the Southern Hemisphere polar region) the temperature at 70 hPa and the near surface CR covariate in *anti-phase*. At other latitudes, however, there is no systematic relation between both variables [14]. On the other hand, comparison with the lower stratospheric ozone's seasonal variations reveals a well pronounced anti-correlation at all examined latitudes (see Fig. 2). The winter reduction of NMs' counting rates, when the ozone density at 70 hPa is raised, is easily noticeable in both hemispheres (Fig. 2). The maximal amplitude of 2.75% is observed at 60°N latitude. It gradually decreases poleward (being 2.3% at 70°N latitude) and toward the equator – dropping to 1% at 20°N latitude. The weakening of the seasonal variability of the ground level CR flux could be attributed to the higher elevation of ozone layer at tropical and subtropical latitudes, and its inability to influence the layer of maximal $\pi$-meson production – placed near 15 km.

In the Southern Hemisphere the number of CR detectors is much lower, but the calculated amplitude of seasonal variation at 45°S latitude is equal to that found at 40°–50°N ones (i.e. 1.5%). The higher amplitude of seasonal variability – found in the NM rates at the surface of the Ice Cube in Antarctica, i.e. 5% [15] – should probably be attributed to the higher elevation of the detector, which is placed at 2835 m above sea level.

These results suggest that the lower stratospheric influence on the NMs' measurements is conducted not through its temperature (as currently believed), but rather through its chemical composition (with a particular importance of the $O_3$molecules, which by the way determine the local temperature outside the polar regions – through an absorption of incoming solar electromagnetic radiation). This suggestion is supported by the fact that the atmospheric $\pi$-*mesons* (called usually *pions*) are produced generally in altitudinal range 10–20 km, which fairly well coincides with the ozone layer [15] at middle and high latitudes. This coincidence could be attributed to the higher radius of the ozone molecule, which increases the *interaction cross-section* of nucleons in the CR atmospheric showers $\sigma_N^{air}$, and consequently a reduction of their mean free path in the atmosphere (see Eq. 2).

$$\lambda_N = \frac{1}{n \cdot \sigma_N^{air}} \tag{2}$$

$n$ in the above equation is the number density of the air. Thus in a region with an increased $O_3$ density the mean free path of energetic nucleons would become smaller than the mean pions free path before their decay (due to the well-defined increase of the $\sigma_N^{air}$ with the growth of the nucleus' geometrical cross-section [16]. In this case the pions' decay is suppressed due to their more frequent interactions with the atmospheric molecules. The tertiary, quaternary, etc. produced pions – due to such interactions – are already less energetic and their probability to reach the surface and to influence the NM measurements is highly reduced [13].

This reasoning could explain the seasonal *anti-phase* covariance between the lower stratospheric $O_3$ and most of the analysed neutron monitors. However, in some of them (i.e. Newark, Dourbes, Rome, Athens, Tsumeb and Potchefstroom) we have found an *in-phase* covariance with ozone at 70 hPa (see Fig. 3). Reference to Fig. 1 reveals that all these "exceptional" NMs are situated in regions with a near zero or very small longitudinal geomagnetic gradient. So with not a great error we can use the dipole estimations of the Regener-Pfotzer maximum's height [17], which in these stations is placed *beneath* 70 hPa. Moreover, the ozone peak layer increases toward the equator, being elevated at sub-tropical latitudes up to the 30 hPa. This means that ozone influence on the layer with higher *pions'* density progressively decreases at lower latitudes.

Consequently, the synchronous *in-phase* variability of the $O_3$ and NMs' counting rates at sub-tropical latitudes is more likely influenced by the atmospheric density seasonal variations, i.e. by the winter compression and summer expansion of the troposphere. Thus the summer uplifting of the denser, and poor of $O_3$, atmosphere will reduce the ozone density in the lower stratosphere. Moreover, the increased density at stratospheric levels will reduce the nucleons' mean free path due to the more frequent interaction with atmospheric molecules (refer to Eq. 2). This means that most of the lower stratospheric pions will not succeed to decay to muons and NMs will encounter a decrease of the muonic component of the ground level CR flux. A weak echo of this effect is visible also at some neutron monitors, shown in Fig. 2. Conversely, the winter compression of the troposphere, followed by a reduction of atmospheric density in the lower stratosphere, will favour the muons production from the $\pi$-mesons decay. In this context, the hemispherical asymmetry visible in Fig. 3, should be attributed to the phase shift of seasons in both hemispheres.

**Conclusions.** The analysis of the annual mean values of cosmic rays for 2009, determined in 33 neutron monitors, spread over the world, reveals that their spatial distribution is generally determined by the elevation of the observational points above the sea level. A closer look reveals, however, the existence of some irregularities, which could be attributed neither to the elevation, nor to the geomagnetic rigidity of the neutron monitors. We show that these irregularities could be attributed to the *geomagnetic focusing* of the precipitating particles in regions with a positive longitudinal magnetic gradient.

Analysis of the CRs' seasonal variability reveals a great variety of patterns – generally confined to geographic latitudes. Comparative investigation of atmospheric ozone at 70 hPa and NMs' counting rates, reveals that they covariate fairly well – with opposite phases. This result implies that previously suggested connection between lower stratospheric temperature and NMs' counting rates are more likely due to the variations of the lower stratospheric composition, and particularly – to the $O_3$ density. The latter possibly affects the muons' production from the $\pi$-mesons' decay in the lower stratosphere.

These results suggest that the amplitude of the ground level enhancement of CR intensity, registered by the ground based NMs (i.e. [18, 19]), is not uniformly distributed over the globe. Having in mind the CR influence on some meteorological parameters [20] it becomes clear that a re-assessment of the factors affecting the production of CR secondaries in the lower atmosphere, similar to that presented in [21] is necessary.

**Acknowledgements.** We acknowledge the NMDB database (`www.nmdb.eu`), founded under the European Union's FP7 programme (contract no. 213007), as well as the IZMIRAN neutron monitors data base (`http://cr0.izmiran.ru/common/links.htm`) for the data provided. Special thanks also to the project teams of ERA Interim reanalysis, providing gridded data for meteorological variables.

## REFERENCES

[1] Selesnick R. S., M. D. Looper, R. A. Mewaldt (2007) A theoretical model of the inner proton radiation belt, Space Weather, **5**, S04003, doi:10.1029/2006SW000275.

[2] Lazutin L. L. (2010) Belt of Protons 1–20 MeV at L = 2, Cosmic Research, **48**(1), 108–112.

[3] Duperier A. (1941) The seasonal variations of cosmic-ray intensity and temperature of the atmosphere, Proc. R. Soc. Lond. A, **177**, 204–216, doi: 10.1098/rspa.1941.0007

[4] Duperier A. (1949) The Meson Intensity at the Surface of the Earth and the Temperature at the Production Level, Proc. Phys. Soc. (A), **62**, 684–694.

[5] Trefall H. (1955) On the Positive Temperature Effect in the Cosmic Radiation and the p-e Decay, Proc. Phys. Soc. (A), **68**, 893–904.

[6] De Mendonça R. R. S., J.-P. Raulin, E. Echer, V. S. Makhmutov, G. Fernandez (2013) Analysis of atmospheric pressure and temperature effects on cosmic ray measurements, J. Geophys. Res., **118**, 1403–1409, doi:10.1029/2012JA018026

[7] Hakkinen L. V. T., T. I. Pulkkinen, R. J. Pirjola, H. Nevanlinna, E. I. Tanskanen, N. E. Turner (2003) Seasonal and diurnal variation of geomagnetic activity: Revised Dst versus external drivers, J. Geophys. Res., **108**(A2), 1060, doi:10.1029/2002JA009428

[8] Velinov P. I. Y. (1968) On ionization of the ionospheric D-region by galactic and solar cosmic rays. J. Atmos. Terr. Phys., **30**(11), 1891–1905.

[9] Velinov P. I. Y., G. Nestorov, L. I. Dorman (1974) Cosmic Ray Influence on the Ionosphere and on Radiowave Propagation, Sofia, Publishing House of Bulgarian Academy of Sciences, 314 pp.

[10] Velinov P. I. Y., L. Mateev (1990) Effects of galactic cosmic rays and high energy particles on the parameters of the global atmospheric electrical circuit, Geomagnetism and Aeronomy, **30**(4), 554–557.
[11] Mateev L., P. I. Y. Velinov (1992) Cosmic ray variation effects on parameters of the global atmospheric electric circuit, Adv. Space Res., **12**(10), 353–356.
[12] Battistoni G., A. Ferrari, M. Pelliccioni, R. Villari (2004) Monte Carlo calculation of the angular distribution of cosmic rays at flight altitudes, Radiat. Prot. Dosimetry, **112**, 331–343. `https://doi.org/10.1093/rpd/nch418`.
[13] Cecchini S., M. Spurio (2012) Atmospheric muons: experimental aspects, Geosci. Instrum. Method. Data Syst., **1**, 185–196.
[14] Kilifraska N., R. Bojilova, Ts. Velichkova (2018) Spatial heterogeneity of cosmic radiation measured at Earth's surface, Proceedings of XIV Intern. conference: "Space, Ecology, Safety", Sofia, 7–9 November 2018, 95–100, p-ISSN 2603–3313, e-ISSN 2603–3321.
[15] Tilav S., P. Desiati, T. Kuwabara, D. Rocco, F. Rothmaier, M. Simmons, H. Wissing (2009) Atmospheric Variations as observed by IceCube 4.
[16] Grieder P. K. F. (2010) Extensive Air Showers: High Energy Phenomena and Astrophysical Aspects – A Tutorial, Reference Manual and Data Book. Springer Science & Business Media.
[17] Sarkar R., S. K. Chakrabarti, P. S. Pal, D. Bhowmick, A. Bhattacharya (2017) Measurement of secondary cosmic ray intensity at Regener-Pfotzer height using low-cost weather balloons and its correlation with solar activity, Advances in Space Research, **60**, 991–998. `https://doi.org/10.1016/j.asr.2017.05.014`
[18] Velinov P. I. Y. (2016) On the distribution of Ground Level Enhancement (GLE) events during solar cycles 17–24, C. R. Acad. Bulg. Sci., **69**(7), 897–904.
[19] Velinov P. I. Y., Yu. V. Balabin, E. A. Maurchev (2017) Calculations of enhanced ionization in strato-troposphere during the greatest Ground Level Enhancement on 23 February 1956 (GLE05), C. R. Acad. Bulg. Sci., **70**(4), 545–554.
[20] Eroshenko E., P. I. Y. Velinov, A. Belov, V. Yanke, E. Pletnikov et al. (2010) Relationships between neutron fluxes and rain flows, Adv. Space Res., **46**, 637–641.
[21] Velinov P. I. Y., N. Smirnova, V. Vlascov (1984) Hybrid quadri-ionic model of the low ionosphere, Adv. Space Res., **4**(1), 123–130.

*National Institute of Geophysics,*
*Geodesy and Geography*
*Bulgarian Academy of Sciences*
*Acad. G. Bonchev St, Bl. 3*
*Sofia 1113, Bulgaria*
*e-mail*: `nkilifarska@geophys.bas.bg`